

See discussions, stats, and author profiles for this publication at: <https://www.researchgate.net/publication/223737171>

# Magnetic anomaly detection using entropy filter

Article in *Measurement Science and Technology* · April 2008

DOI: 10.1088/0957-0233/19/4/045205

---

CITATIONS

25

---

READS

626

5 authors, including:



**Arie Sheinker**

Soreq Nuclear Research Center

18 PUBLICATIONS 301 CITATIONS

[SEE PROFILE](#)



**Boris Ginzburg**

Soreq Nuclear Research Center

22 PUBLICATIONS 387 CITATIONS

[SEE PROFILE](#)

# Magnetic anomaly detection using entropy filter

Arie Sheinker<sup>1,2</sup>, Nizan Salomonski<sup>1</sup>, Boris Ginzburg<sup>1</sup>, Lev Frumkis<sup>2</sup> and Ben-Zion Kaplan<sup>2</sup>

<sup>1</sup> R&D Integrated Systems Section, Propulsion Division, SOREQ NRC, Yavne 81800, Israel

<sup>2</sup> Department of Electrical and Computer Engineering, Ben-Gurion University of the Negev, Beer-Sheva 84105, Israel

E-mail: [sheinker@ee.bgu.ac.il](mailto:sheinker@ee.bgu.ac.il)

Received 21 November 2007, in final form 28 January 2008

Published 25 February 2008

Online at [stacks.iop.org/MST/19/045205](http://stacks.iop.org/MST/19/045205)

## Abstract

We address the detection of a ferromagnetic target that generates an anomaly in the ambient Earth magnetic field. Detection of an anomaly buried in magnetic noise requires the use of a magnetic anomaly detector (MAD), such as the orthonormal basis functions (OBFs) detector. In contrast to the OBFs detector that relies on target signal waveform ensemble, we propose the adaptive **minimum entropy detector** (MED) to detect any changes in the magnetic noise pattern. Hence, we have constructed the MED based on the magnetic noise probability density function. The MED was tested on real-world magnetic noise and compared to the OBFs detector. Higher detection rate was exemplified for the MED over the OBFs detector in detecting a ferromagnetic target with low signal-to-noise ratio (SNR). Appreciable advantage of the MED over the OBFs detector is shown, when the target does not move according to the assumed pattern. The low-computational complexity makes the MED appropriate for real time applications.

**Keywords:** entropy, magnetometer, magnetic anomaly detection (MAD), magnetic noise, orthonormal basis functions (OBFs)

## 1. Introduction

A wide range of applications exploit the magnetic field for detection [1], localization [2] and tracking [3] of visually obscured targets. A ferromagnetic target produces a magnetic field, which farther from the target is assumed to be a magnetic dipole field [4],

$$\vec{B}(\vec{m}, \vec{r}) = \frac{\mu_0}{4\pi} \left[ \frac{3(\vec{m} \cdot \vec{r})\vec{r}}{|\vec{r}|^5} - \frac{\vec{m}}{|\vec{r}|^3} \right] + \vec{B}_E. \quad (1)$$

The target magnetic moment is denoted by  $\vec{m}$  and  $\vec{r}$  is the distance between the target and the sensor. The target magnetic field appears as an anomaly in the ambient Earth magnetic field  $\vec{B}_E$ . Magnetic anomaly detectors (MAD) are used to detect the anomaly which is usually contaminated by magnetic noise. In contrast to methods that rely on possible target signal waveforms, such as the orthonormal basis functions (OBFs) detection method [5], **we propose an adaptive minimum entropy detector (MED), which detects any**

**change in the magnetic noise pattern. In many cases the real-world magnetic noise has a normal probability density function, which is governed by the mean and variance parameters.** The density function is derived by sampling the magnetic noise and using the samples to calculate the mean and variance. Using the estimated magnetic noise density function, the probability of each sample can be evaluated. The entropy [6] is calculated using the probabilities of samples in a moving window. **Existence of a magnetic anomaly is revealed by a drop in the entropy value below a threshold.** The MED was tested on a real-world magnetic noise acquired by a fluxgate magnetometer, and **compared to the OBFs detector. Higher detection rate was exemplified for the MED over the OBFs detector in detecting anomalies with low SNR.** Appreciable advantage of the MED over the OBFs detector is shown, when the target does not move according to the assumed pattern. The low-computational complexity makes the MED appropriate for real time applications, such as monitoring changes in the Earth magnetic field, and intruder detection.

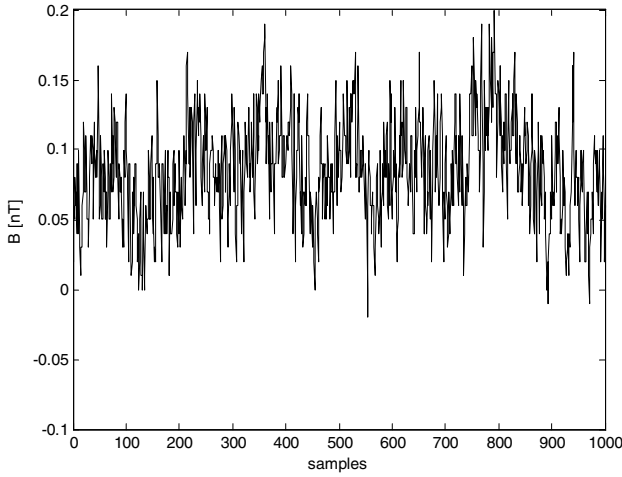


**Figure 1.** A real-world magnetic noise acquired by a LEMI-019 single-axis fluxgate magnetometer. The magnetometer output was sampled at a rate of 10 samples per second.

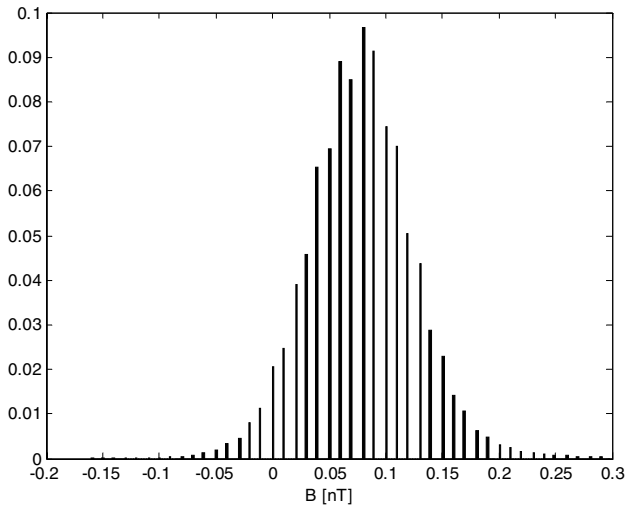


**Figure 2.** The normalized histogram of an acquired magnetic noise approximates a normal probability density function. The calculated mean and variance are 0.07 nT and 0.002 nT<sup>2</sup>, respectively.

## 2. Magnetic noise distribution

A real-world magnetic noise was acquired for about 12 h by the LEMI-019 [7] single-axis fluxgate magnetometer [8, 9] in a comparably quiet magnetic surrounding. The magnetometer has an internal band pass filter (BPF) in the frequency range of 0.02–5 Hz, with intrinsic noise of less than 15 pT/ $\sqrt{\text{Hz}}$  at a frequency of 1 Hz. The magnetometer output was sampled with a sampling period  $T_s$  of 0.1 s. We aligned the magnetometer with the Earth magnetic field direction, which results in readings that resemble a total field magnetometer [10]. Figure 1 shows a typical segment of a thousand readings from the acquired magnetic noise, which mainly consists of external geomagnetic noise and intrinsic sensor noise [11].

The histogram of a measured noise when normalized by the number of samples is close to the normal probability density function as depicted in figure 2.

For a sample  $x_i$ , the normal probability density function is governed by the mean  $\mu$  and the variance  $\sigma^2$

$$f(x_i) = \frac{1}{\sqrt{2\pi\sigma^2}} \exp \left\{ -\frac{(x_i - \mu)^2}{2\sigma^2} \right\}. \quad (2)$$

The mean and variance can be estimated by  $M$  samples using

$$\mu = \frac{1}{M} \sum_{i=1}^M x_i, \quad \sigma^2 = \frac{1}{M} \sum_{i=1}^M (x_i - \mu)^2. \quad (3)$$

For the acquired magnetic noise of a total of  $M = 432\,000$  samples, the calculated mean and variance are 0.07 nT and 0.002 nT<sup>2</sup>, respectively. The probability of a noise sample taking a discrete value of  $x_i$  is given by

$$p(x_i) = \int_{x_i}^{x_i + \Delta x} f(x_i) dx_i. \quad (4)$$

Since we use an analog-to-digital converter with a quantization step  $\Delta x$ , the probability  $p(x_i)$  can be approximated by

$$p(x_i) \cong f(x_i) \Delta x. \quad (5)$$

For the analog-to-digital converter in use the quantization value is about 0.01 nT.

## 3. The entropy filter

The anomaly in the measured magnetic field which is produced by a ferromagnetic target changes the magnetic noise pattern. Entropy is a basic concept of information theory which is usually used as a measure of information [12]. We used it to detect the changes in the magnetic noise pattern. The entropy filter calculates the entropy in a moving window of  $L$  samples according to

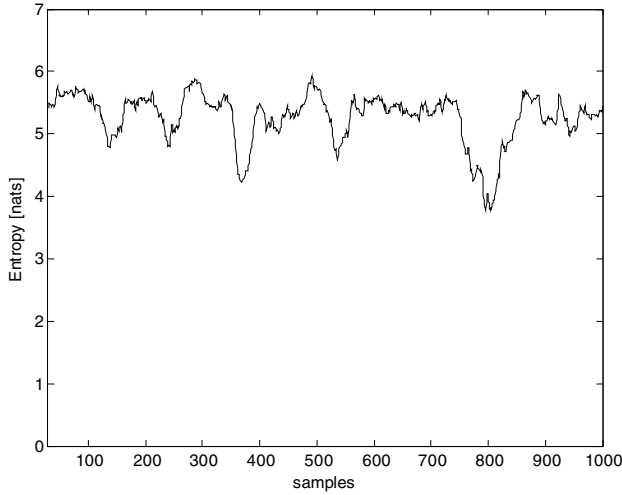
$$I(x_i) = - \sum_{n=i-L+1}^i p(x_n) \log p(x_n). \quad (6)$$

We chose to use the natural logarithm, and therefore the units of entropy are nats.

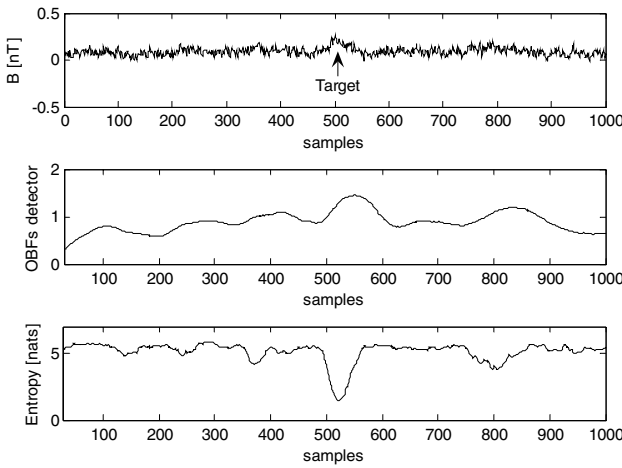
The MED consists of an entropy filter and a threshold, thus, detection occurs whenever the entropy filter output drops below threshold value. After several experiments the entropy filter length  $L$  was set to 30 samples, nonetheless, tests indicate that the entropy filter can operate well with a wide range of length values. Figure 3 shows the output of the entropy filter calculated on the magnetic noise shown in figure 1.

Figure 4 shows a signal of a magnetic target on the background of a real-world magnetic noise, and the response of the entropy filter. The SNR at the input is clearly much smaller than the SNR at the output, indicating significant improvement in detection ability.

In order to evaluate the MED detection rate we have performed a statistical test. With this end in view, the entropy filter was applied to the acquired noise samples and the response was recorded. Normalizing the recorded filter response by the number of samples yields the noise *a posteriori* probability after filtering. Afterward, 10 000 windows were chosen randomly out of the acquired magnetic noise, and a



**Figure 3.** The entropy filter output for the real-world magnetic noise in figure 1.



**Figure 4.** A signal of a target with a magnetic moment of  $0.06 \text{ A} \cdot \text{m}^2$  aligned with the Earth magnetic field, contaminated by real-world magnetic noise (top). The target moved along a straight line toward the sensor and then returned, reaching a CPA of 3 m. The target signal is barely distinguished by the OBFs detector (middle), but clearly detected by the entropy filter (bottom).

target signal was added to each chosen window. We chose a target track along a straight line from south to north, passing by the sensor. The entropy filter was applied to each chosen window and the response was recorded. Normalizing the recorded filter response by the total number of windows yields the target *a posteriori* probability after filtering. Figure 5 shows both noise and target *a posteriori* probabilities after filtering. The threshold value is determined using the Neyman–Pearson criterion [13] for achieving maximal detection probability under a constraint on the false alarm rate. This criterion is useful in the case of unknown target *a priori* probability, e.g. intruder detection scenario. We chose a false alarm rate of 4%, which results in a threshold value of 2.9 nats that provides a detection probability of 94%.

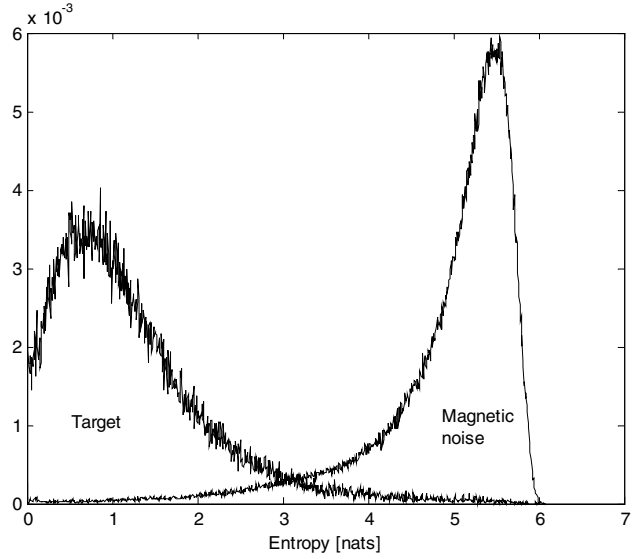


**Figure 5.** The *a posteriori* probabilities of both noise and target after filtering. The target with a magnetic moment of  $0.06 \text{ A} \cdot \text{m}^2$  aligned with the Earth magnetic field was moved along a south–north track with CPA of 3 m, resulting in SNR of  $-5 \text{ dB}$ .

#### 4. Comparison with orthonormal basis functions detector

Consider a static total field magnetometer as depicted in figure 6, which measures the magnetic field generated by a target moving along a straight line. The characteristic time  $\tau$  is defined as the CPA divided by target velocity, where CPA is the closest proximity approach. Using the Gram–Schmidt procedure, the target signal can be represented as a linear combination of three orthonormal basis functions. In discrete-time form the OBFs are represented as three sequences in the range  $-N \leq n < N$ ,

$$\begin{aligned} f_1(n) &= \sqrt{\frac{24}{5\pi}} \frac{1 - \frac{5}{3}(nT_s/\tau)^2}{[1 + (nT_s/\tau)^2]^{2.5}} \\ f_2(n) &= \sqrt{\frac{128}{5\pi}} \frac{nT_s/\tau}{[1 + (nT_s/\tau)^2]^{2.5}} \\ f_3(n) &= \sqrt{\frac{128}{3\pi}} \frac{(nT_s/\tau)^2}{[1 + (nT_s/\tau)^2]^{2.5}}. \end{aligned} \quad (7)$$

In order to concentrate most of the OBFs energy,  $N$  should be larger than  $\tau/T_s$ , but not too large to avoid picking up extra noise. It is recommended that  $N$  will be smaller than  $1.5\tau/T_s$ . Usually, neither target velocity nor CPA are known *a priori*. Thus, in order to build the OBFs in equation (7), either characteristic time value should be guessed or a multi-channel approach should be adopted.

The detector consists of three matched filters [5], each corresponding to one of the OBFs. The digital implementation of the OBFs detector is depicted in figure 7.

For the derivation of the OBFs we must rely on several assumptions about the target: the target is represented by a single magnetic dipole model, the target moves along a straight line passing by the sensor, the target characteristic time is known *a priori*. The MED is beneficial in being independent

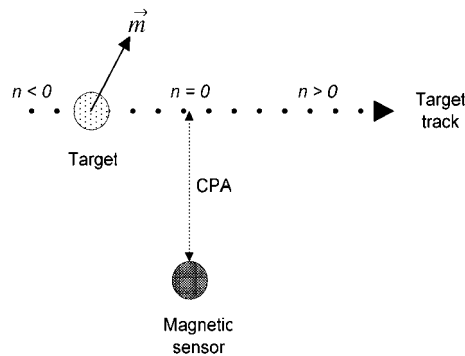


**Figure 6.** A magnetic target moves along a straight line passing by a static magnetometer.

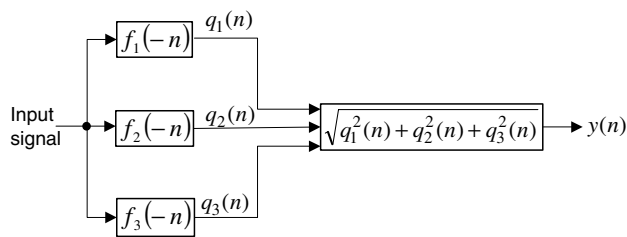


**Figure 7.** The digital implementation of the OBFs detector.

of those assumptions because in practise they are not always fulfilled. In figure 4, there is an example of a signal of a target moving toward a sensor and then returning back. The target signal is barely distinguished by the OBFs detector, but clearly detected by the entropy filter.

It is important to note that the MED is based on noise characteristics, whereas the OBFs detector relies on target signal pattern. This is the reason for the OBFs detector being more immune to magnetic interferences which are not of the form of (1). On the other hand, for the MED, gradiometric compensation of far origin interference is more essential.

The matched filter is proved to be optimal with Gaussian (normal) white noise. However, the magnetic noise power spectral density can take the form of  $1/f^\alpha$ , where  $\alpha$  slowly varies with time [11]. Usually, only an approximate whitening filter is available which should be recalculated periodically [10]. In contrast, the only assumption for the MED is a normal probability density function of the magnetic noise, which practically holds in many cases as shown in figure 2. Another advantage of the MED is its low computational complexity compared with the OBFs detector. The OBFs detector output at every instant is calculated by a sum of three convolutions, each convolution is calculated by a sum of multiplications, which is a time-consuming operation. On the other hand, every output value of the MED is calculated using a sum of terms, in the form of  $p(x_i) \log p(x_i)$ , where each term can be read from a look-up table that was prepared earlier. The changing environmental conditions can influence the magnetic noise characteristics. Hence, it is necessary to update the look-up table periodically using (3), in order to properly adapt the detector.

Finally, we compared the detection probability of the MED and the OBFs detector. The OBFs detector has passed

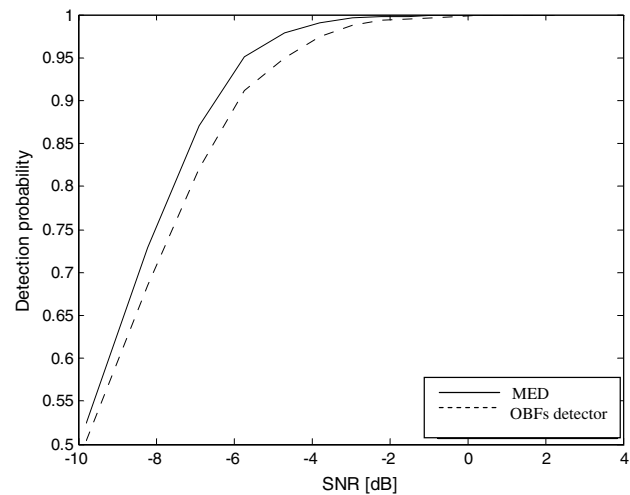


**Figure 8.** The detection probabilities of the MED versus the OBFs detector. We have used the *a priori* known target characteristic time for the OBFs detector. The threshold value was set using the Neyman–Pearson criterion for false alarm rate less than 4%.

the same test as described above for the MED. Figure 8 shows the detection probability evaluated using the Neyman–Pearson criterion for various values of SNR. We see that even for the best case of the OBFs detector with *a priori* known target characteristic time, the MED achieves higher detection probability for the described measurement scenario.

## 5. Conclusions

We have developed a magnetic anomaly detector based on an entropy filter. The detector calculates and examines the entropy of the magnetic noise in a moving window. Detection occurs whenever the entropy drops below a threshold value, which was determined using the Neyman–Pearson criterion. Tests with real-world magnetic noise exemplify higher detection probability of the MED over the fundamental OBFs detector. The advantage of the MED is even more prominent when a target does not move according to an anticipated pattern. The low computational complexity makes the MED attractive for real-time applications.

Further research will address the optimization of adapting the MED to changes in environmental conditions.

## Acknowledgments

We would like to thank Mrs Avivit Noiman, Mr Yosef Elek and Mr Yohai Nitzan, for their important technical support.

## References

- [1] Ginzburg B, Frumkis L and Kaplan B Z 2004 An efficient method for processing scalar magnetic gradiometer signals *Sensors Actuators A* **114** 73–9
- [2] Marschner U and Fischer W J 2007 Indirect measurement of a bar magnetic position using a Hall sensor array *IEEE Trans. Magn.* **43** 2728–30

- [3] Paperno E, Sasada I and Leonovich E 2001 A new method for magnetic position and orientation tracking *IEEE Trans. Magn.* **37** 1938–40
- [4] Blakely R J 1996 *Potential Theory in Gravity and Magnetic Applications* (Cambridge: Cambridge University Press) pp 75–9
- [5] Ginzburg B, Frumkis L and Kaplan B Z 2002 Processing of magnetic scalar gradiometer signals using orthonormalized functions *Sensors Actuators A* **102** 67–75
- [6] Hyvarinen A, Karhunen J and Oja E 2001 *Independent Component Analysis* (New York: Wiley) pp 105–20
- [7] LEMI-019 Lviv Centre of Institute of Space Research, Ukraine, <http://www.isr.lviv.ua/lemi019.htm>
- [8] Ripka P 2001 *Magnetic Sensors and Magnetometers* (Boston, MA: Artech House) pp 75–120
- [9] Ripka P 2003 Advances in fluxgate sensors *Sensors Actuators A* **106** 8–14
- [10] Sheinker A, Shkalim A, Salomonski N, Ginzburg B, Frumkis L and Kaplan B Z 2007 Processing of a scalar magnetometer signal contaminated by  $1/f^\alpha$  noise *Sensors Actuators A* **138** 105–11
- [11] Korepanov V and Berkman R 1999 Fluxgate magnetometer noise: theoretic and experimental study *Proc. 3rd Biennial Conf. on Measurements for a Sustainable Future MSA99 (Sydney, Australia)* pp 41–4
- [12] Bercher J F and Vignat C 2000 Estimating the entropy of a signal with applications *IEEE Trans. Signal Process.* **48** 1687–94
- [13] McDonough R N and Whalen A D 1970 *Detection of Signals in Noise* (New York: Academic) pp 159–66